

Article

Development of the nonlinearity correction for the laser tuning in OFDR system using zero-crossing sampling and self-reference

Shiyuan Zhao ^{1,2,3}, Jiwen Cui ^{1,2,*} and Jiubin Tan ^{1,2}¹ Center of Ultra-precision Optoelectronic Instrument, Harbin Institute of Technology, Harbin, 150080, China² Key Lab of Ultra-precision Intelligent Instrumentation (Harbin Institute of Technology), Ministry of Industry and Information Technology, Harbin, 150080, China³ Email: zhshy776127227@163.com

* Correspondence: cuijiwen@hit.edu.cn; Tel.: 86-451-86412041

Abstract: Tuning nonlinearity of the laser is the main source which will deteriorate the spatial resolution in optical frequency domain reflectometry system. We develop methods for tuning nonlinearity correction in the OFDR system from the aspects of data acquisition and also the post-processing. A zero-crossing detection scheme is researched and implemented by a customized circuit. Equal-spacing frequency sampling is therefore achieved in real-time. The maximum sensing distance can reach to the same length of the auxiliary interferometer. The zero-crossing detection for the beating frequency of 20MHz is achieved. Then, a nonlinearity correction method based on the self-reference method is proposed. The auxiliary interferometer is no longer necessary in this scheme. The tuning information of the laser is extracted by a strong reflectivity point at the end of the sensing arm in the main interferometer. The tuning information can then be used to resample the raw signal and the nonlinearity correction can be achieved. The spatial resolution test and the distributed sensing experiments are both performed based on this nonlinearity correction method. The results validated the feasibility of the proposed method. The method reduces the hardware and data burden for the system and has a potential value on the system integration and miniaturization.

Keywords: optical fibers; Rayleigh scattering; optical frequency-domain reflectometry; strain measurement

1. Introduction

Optical frequency domain reflectometry (OFDR) based distributed sensing system was initially proposed by Froggatt et al. in 1998 and utilized in distributed disturbance such as strain or temperature measurement because of its high spatial resolution and sensitivity [1-3]. In an OFDR system, the interference signals are collected as a function of optical frequency of a tunable laser source (TLS). A Fast Fourier transform (FFT) is then used to convert this frequency domain information to a desired spatial information, where it requires that the interference signals are sampled at an equal interval of the optical frequency [4]. However, any frequency tuning nonlinearity of a TLS gives a rise of non-uniform sampling interval of the optical frequency when the signal is sampled by an equal time interval which, in turn, results in spreading of the reflection peak energy, deteriorating the spatial resolution [4].

Two kinds of methods are developed in recent years to solve the problem of the laser tuning nonlinearity. The first is to utilize an auxiliary interferometer to produce an external sampling clock as data acquisition trigger [5]. Although this method is real-time and does not need the post-processing, a drawback of this method is that the maximum measurement length is limited by the optical path difference (OPD) between the two arms of the auxiliary interferometer that is four times

the sensing fiber length in order to satisfy the Nyquist Law [6]. This does limit the sensing range of the system. Some researches proposed using inphase quadrature detection (IQ) such as the 3×3 coupler [7] or optical hybrid receiver [8], which can double the detection length. However, in these schemes, the complex operation in the demodulation is introduced which would decrease the real-time demodulation of the system.

The second method to correct the tuning nonlinearity is to perform post signal processing after acquiring OFDR data. Normally, this technique involves acquiring an auxiliary interferometer signal along with the OFDR and extracting the TLS phase information from the auxiliary interferometer signal and compensating nonlinearity in the OFDR signal using a correction algorithm [4]. One of the algorithms is the resampling technique that resamples the main beating interference signals with an accurate equidistant optical frequency grid based on the optical frequency information of the TLS by the interpolation algorithms. Mudabbir Badar et al. proposed a self-correction scheme which only one detector is contained in the measurement system. In their proposed scheme, an intentional beating signal is introduced at the beginning of the OFDR spectrum which is treated as an auxiliary interferometer to acquire tunable laser phase information for post signal processing [9]. However, two drawbacks exist in their scheme. One is an extra delay for the intentional beating signal is induced in the system, which will increase the instability. The other is the intentional beating signal is at the beginning of the spatial domain. This design makes the OPD of the main interferometer is much longer than the auxiliary interferometer. Therefore, much interpolation has to be implemented which will increase the probability of false information, and also significantly increase the data volume. What else, the intentional beating signal will occupy one segment at low-frequency position, which will sacrifice a part of effective sensing distance.

In this paper, the tuning nonlinearity correction methods in OFDR system are developed from the aspects of data acquisition and also the post-processing. On one hand, a new hardware-based method for real-time equal frequency interval sampling is presented, which is implemented by designing an external clock to provide triggers at zero-crossing positions with uniform frequency spacing. The limited sensing distance which is one half of the OPD of the auxiliary interferometer in the conventional OFDR acquisition mode can double and extend to the same length with the OPD of the auxiliary interferometer. On the other hand, the resampling method for tuning nonlinearity correction based on single main interferometer and self-reference is demonstrated. The frequency tuning information of the laser is obtained from the PC connector at the end of the measurement arm. In this case, no extra delay fiber is needed because the sensing fiber also plays the role of the optical path of the PC-constituted interferometer. What else, since the PC connector is at the end of the measurement arm, the OPD of the PC-constituted interferometer is longer than the main interferometer. That is, the beating frequency of the PC connector is larger than that of reflectivity points before the PC connector which is also served as the sensing part. Therefore, in the algorithm which will be demonstrated later, it does not need much phase subdivision to resample the fringe signal which makes the effect of the nonlinearity correction more stable. Generally, a phase increment π or $\pi/2$ can meet the nonlinearity correction requirement and the maximum sensing distance will not lower than the OPD of the PC connector.

The rest of this paper is organized as follows. Section 2 describes the principle of the zero-crossing detection method. The circuit design and scheme are demonstrated. The method is validated from the spatial resolution and maximum sensing distance. Section 3 demonstrates the method of nonlinearity correction using the self-reference. Section 4 concludes this paper.

2. Zero crossing detection-based external clock

2.1 Method description

Ignoring the phase noise of the laser, the interference pattern of the auxiliary interferometer with a Mach-Zehnder scheme can be written as Equation (1).

$$I_a = \cos[2\pi\gamma(t)\tau_a t + \phi_0] \quad (1)$$

In Equation (1), $\gamma(t)$ is the tuning speed of the laser. τ_a is the time delay of the Mach-Zehnder interferometer. ϕ_0 is the initial phase. The zero of Equation (1) occur when the phase is

$$2\pi\gamma(t)\tau_a t + \phi_0 = \frac{\pi}{2} + k\pi. \quad (2)$$

In Equation (2), k is an integer.

According to $t = \frac{v(t)}{\gamma(t)}$, where $v(t)$ is the optical frequency, Equation (2) can be written as

$$2\pi v(t)\tau_a + \phi_0 = \frac{\pi}{2} + k\pi. \quad (k=1, 2, \dots) \quad (3)$$

Then,

$$v(t_k) = \frac{\frac{\pi}{2} + k\pi - \phi_0}{2\pi\tau_a}. \quad (4)$$

The optical frequency at the zero-crossing points can be expressed as Equation (5). It can be seen from Equation (5), at each zero-crossing point, the optical frequency increment is equal and related to the position of the OPD of the auxiliary interferometer.

$$v(t_k) = \frac{k}{2\tau_a} + \text{const}. \quad (5)$$

Next, we will analyze the signal of the main interferometer. The interference intensity of the reflectivity point D in the measurement arm with the local light from the reference arm in the main interferometer can be written as

$$I_D = \cos[2\pi v(t)\tau_D + \phi_d]. \quad (6)$$

In Equation (6), τ_D is the time delay between the point D and the local light from the reference arm. ϕ_d is the initial phase. The zero-crossings of the pattern of the auxiliary interferometer can be used to resample the measured beat signal. When resampling to the interference signal I_D with an interval of $\Delta v = \frac{1}{2\tau_a}$, the resampled points can be written as

$$I_{D,M} = \cos\left[\pi \frac{M}{\tau_a} \tau_D + \phi_d\right]. \quad (M=1, 2, \dots) \quad (7)$$

The beating frequency of the auxiliary interferometer and the main interferometer are $f_a = 2\gamma\tau_a$ and $f_D = \gamma\tau_D$, respectively. To satisfy the Nyquist criterion, it requests $f_a > 2f_D$. Then, it requests $\tau_a > \tau_D$. Therefore, the zero-crossing points are used to be the trigger signal, the measurable distance can reach to the distance of the auxiliary interferometer. However, most the commercial DAQ can only sample at the rising OR falling edge if using the external clock mode. This makes that the measurable distance is limited to half of the distance of the auxiliary interferometer.

2.2. Hardware implementation

As the principle demonstrated before, the core task is to design a circuit which can detect the zero-crossing points of the signal of the auxiliary interferometer (AI). Considering the tuning

nonlinearity of the laser, the sinusoidal signal will have a frequency fluctuation centered at its nominal beating frequency. The requirement for the circuit is high speed and low-delay. What else, since the nominal beating frequency depends on the tuning speed of the laser, the maximum frequency of the AI is determined by the required measurement speed of the system. In our system, the maximum frequency of the AI is designed to be 20 MHz. That means the maximum input frequency of the circuit for zero-crossing detection is 20 MHz. The total delay of the circuit should be less than half period of the frequency of the AI signal. With this rule, the trigger signal of the circuit can be considered to track and reflect the changing-frequency AI signal. For the frequency of 20 MHz, the half period is 25 ns. Therefore, it should keep that the final trigger signal has a total delay less than 25 ns in the consideration of the device selection for the circuit.

Figure 1 shows the circuit scheme of the zero-crossing detection for the AI signal. Figure 2(a) gives the signal curves at each node. The AI signal is inverted firstly. Then the original AI signal and its inversion signal are sent into the two comparators, respectively. The output of the comparators will be at the high level alternately with half period of the AI signal. Then the output of the comparators are sent into a XOR gate, after which the pulse will appear at each half period of the AI signal. The differentiation unit is used to convert the pulse to a narrow signal. The position of the rising edge of the trigger signal will appear after the zero-crossing of the AI signal. The time delay ΔT depends on the total time delay of each component in the circuit.

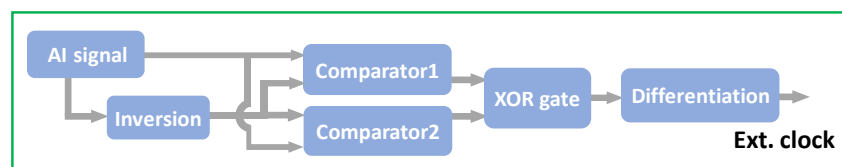


Figure 1. Circuit scheme of the zero-crossing detection for the AI signal

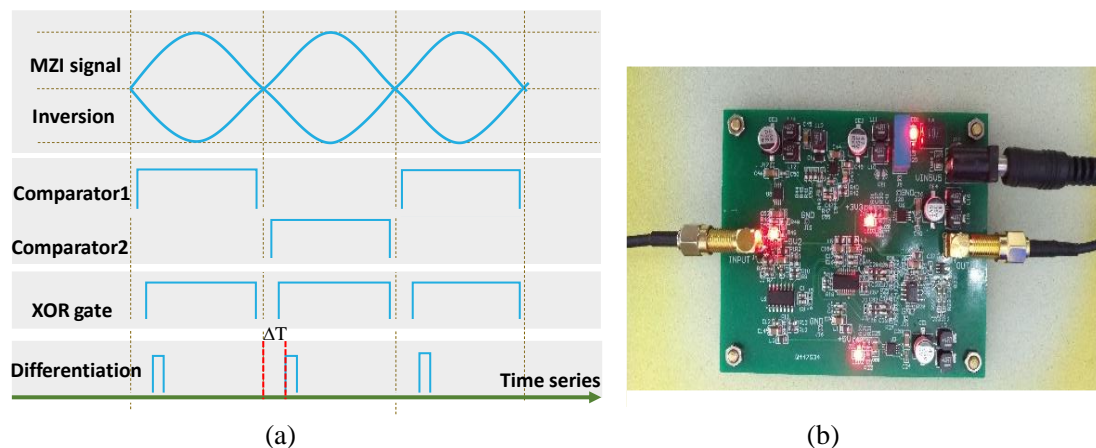


Figure 2. (a) Time series analysis at each node on the circuit. (b) Photograph of the circuit board based on the proposed zero-crossing detection scheme.

2.3. Experiment

A conventional OFDR system is shown in Figure 3. The light from the laser (Phoenix 1400 from LUNA corporation, 3 MHz linewidth) is split into two paths by a 10:90 optical coupler. 10 % light is sent to an auxiliary interferometer with a delay fiber of 250 m. The laser sweeps from 1540 nm to 1560 nm so the two-point spatial resolution Δz of the system is 40 μm calculated by $\Delta z = c / 2n\Delta\nu$, where n is the refractive index of FUT, and $\Delta\nu$ is the optical frequency tuning range of the TLS. The customized PCB is added after the PD. The sampling mode of data acquisition card (DAQ) is set to use the rising edge of the external clock as the trigger source.

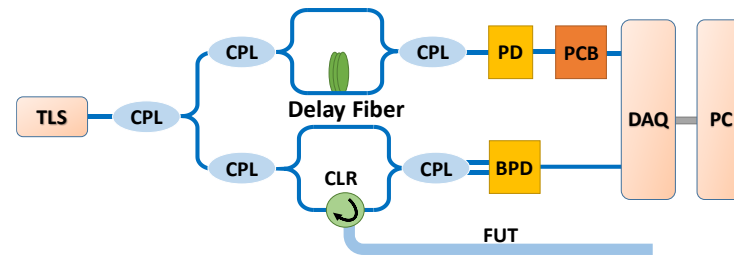


Figure 3. OFDR system. The auxiliary interferometer is an unbalanced Mach-Zehnder interferometer with 250m reference delay fiber. TLS: tunable laser source; CPL: fiber coupler; CLR: fiber circular; BPD: balanced photo detector; DAQ: data acquisition. PC: personal computer.

First, the input-output timing sequence of the customized PCB is tested. Different tuning speed are set so that the nominal beating frequency of the AI is different. The beating frequency satisfies $f_{beat} = \gamma \tau$, where γ is the tuning speed with a unit of Hz/s, and τ is the time delay of the auxiliary interferometer. The tuning speed of 32 nm/s, 80 nm/s and 128 nm/s corresponds to beating frequency of 5 MHz, 12.5 MHz and 20 MHz, respectively. The input-output time sequence are shown in Figure 4. It can be seen that the time delay between the zero-crossing points in AI signal and the trigger signal are within one half period of the AI signal. What's more, the time delay of the trigger signal after the zero-crossing points of the AI signal are almost the same and can be considered to be constant if the time delay difference of the two comparators used in the circuit is negligent.

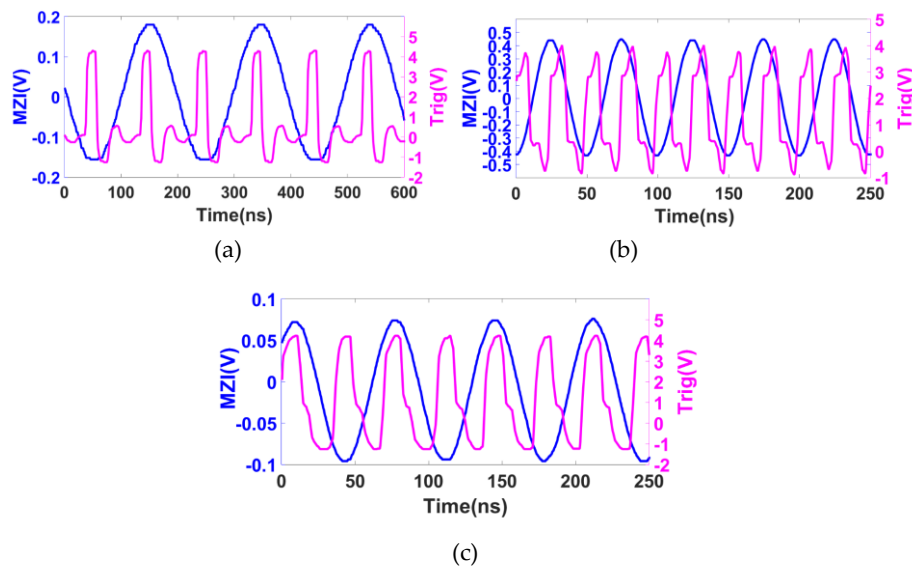


Figure 4. Input-output curve of the PCB for zero-crossing detection at different input frequency. The blue curve is the AI signal and the pink curve is the output trigger signal of the PCB. (a-c) have nominal input frequency of 5MHz, 20MHz and 12.5MHz, respectively.

Then the OFDR trace is sampled by the DAQ with our customized PCB at the condition of 80 nm/s tuning speed. The nominal beating signal of the AI is then 12.5 MHz. The original signal from main interferometer is fast Fourier transformed to the spatial domain. The result is shown in Figure 5. It can be seen that the sensing length can reach to the length which equals to the OPD of the auxiliary interferometer. The -3 dB width of the APC connector is 40 μm , which is the Fourier transform-limited spatial resolution. At the end of the fiber, the -3 dB width of the APC connector decreased to about 3.48 mm. The resolution deterioration mainly comes from the increasing phase noise of the laser which increases with the length.

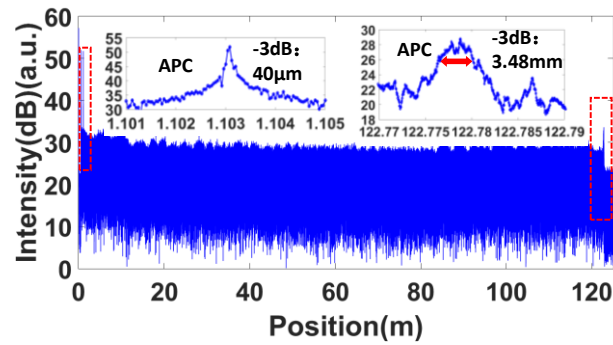


Figure 5. Measured OFDR trace with an APC connector end which immersed into refractive index matching liquid.

3. Nonlinearity correction based on self-reference

3.1 Method description

The detected interference pattern interfered by the strong reflectivity point (e.g. a PC connector) with the local light can be written as

$$I_{pc}(t) = \cos[2\pi\gamma(t)\tau t + \xi_0]. \quad (8)$$

In Equation (8), $\gamma(t)$ is the tuning speed of the laser. τ is the time delay between the PC connector and the local light from the reference arm. ξ_0 is the initial phase. The Hilbert transformation (HT) of $I_{pc}(t)$ can be expressed as

$$HT\{I_{pc}(t)\} = \sin(2\pi\tau v(t) + \xi_0). \quad (9)$$

The phase of the interference pattern is represented as

$$\phi(t) = 2\pi\tau v(t) + \xi_0 = \tan^{-1}[HT\{I_{pc}(t)\} / I_{pc}(t)]. \quad (10)$$

The optical frequency of the laser is

$$v(t) = \frac{1}{2\pi n} \frac{c}{\Delta L} \phi(t), \quad (11)$$

where ΔL is the OPD between the PC connector and the local light from the reference arm. It can be seen from Equation (11), the resampled points at each equal optical phase interval represent equal optical frequency interval.

Figure 6 describes the nonlinearity correction process using the self-reference method. The raw signal in the optical frequency domain is sampled using a fixed sampling rate, then it is converted to the spatial domain by FFT. Then, a rectangle band-pass filter is applied on the data in the spatial domain. The band should cover the peak band of the reference point which may be a PC connector. The reminder of the spectrum are set to zero. After that, the filtered data is inverse fast Fourier transformed back to the optical frequency domain. Then, take the real part of the complex data and make the data be the real number. After that, the Hilbert transformation (HT), arc tangent operation are used to unwrap the phase. Therefore the nonlinearity information has been obtained. Next, the unwrapped phase is divided into equal-spacing segments with an equal phase interval. These positions are then used to resample the raw signal. Finally, the nonlinearity-corrected interferometer signal has been obtained. It should be noted, in the process aforementioned, no interpolation is introduced.

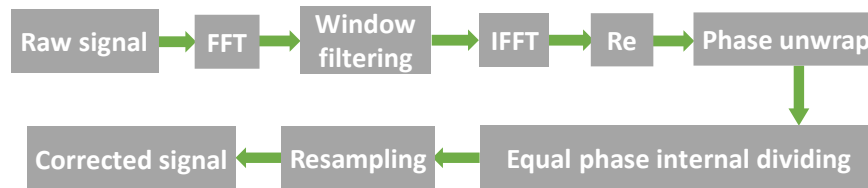


Figure 6. Procedure for the self-reference of laser tuning nonlinearity.

3.2. Simulation

To simply the simulation, we assume that the optical frequency of the laser satisfies the quadratic function which modeled by

$$\nu(t) = \gamma t + at^2, \quad (12)$$

where γ is the tuning speed and a is the nonlinearity coefficient.

The simulation parameters for the tuning process are as follows: Tuning range is 2500 GHz. Tuning speed is 5000 GHz/s. Sampling rate is 10 MS/s. Sampling number is 5 MS. Optical frequency deviation at the middle optical frequency is -1 GHz.

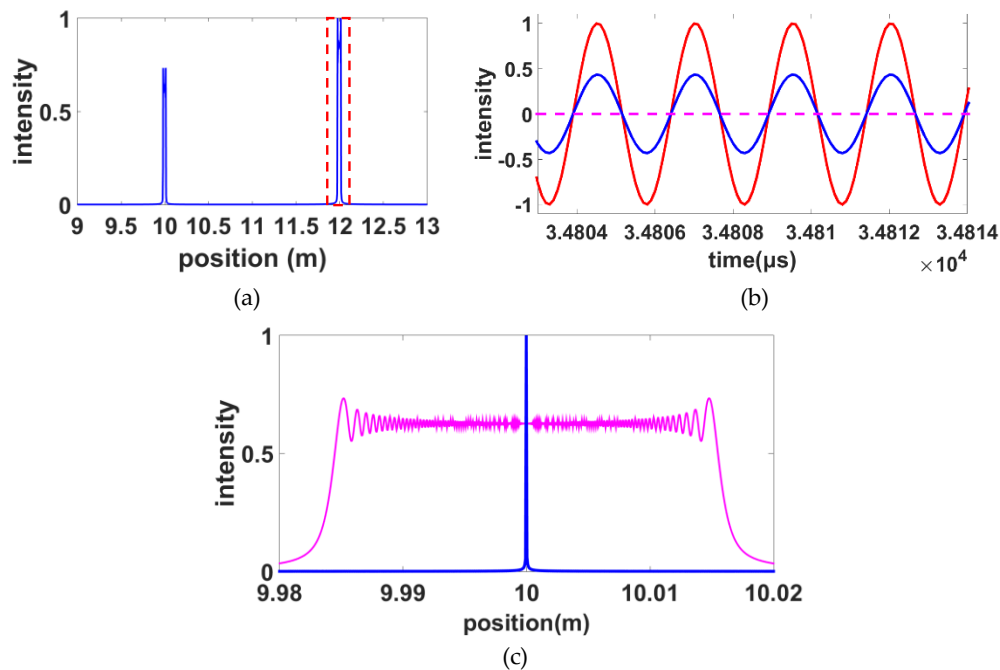


Figure 7. (a) Two reflection peaks in the spatial domain which are broadened by the nonlinearity of the laser. (b) The interference patterns during a period of time. Blue curve is the ideal interference pattern in temporal domain. Red curve is the signal which recovered by the band-pass filtered signal shown in (a). (c) The pink and blue curves are the first reflection peak without and with the nonlinearity correction using the self-reference method. All intensity are normalized.

Two reflection points are simulated and their OPD are 20 m and 24 m. The second reflection point is the reference point used to correct nonlinearity. Figure 7 (a) is the OFDR trace in the spatial domain. It can be seen the peaks are broadened centered at 10 and 12 m. The spatial resolution is deteriorated by the tuning nonlinearity of the laser. In Figure 7 (b), the blue curve is the ideal interference pattern in temporal domain, which is the interference between the ideal reflection at the position of 24 m and the local light. The red curve is the result after taking the real part (without phase unwrap) shown in Figure 6. It can be seen that the recovered interference pattern has the same

phase compared to the ideal interference pattern. Therefore, the self-reference method has the same effect as the conventional auxiliary interferometer shown in Figure 3. Figure 7 (c) compares the results with and without nonlinearity correction using the self-reference method. It can be seen that after the nonlinearity correction using the self-reference method, the Fourier transform-limited spatial resolution can be achieved.

3.3. Experiment

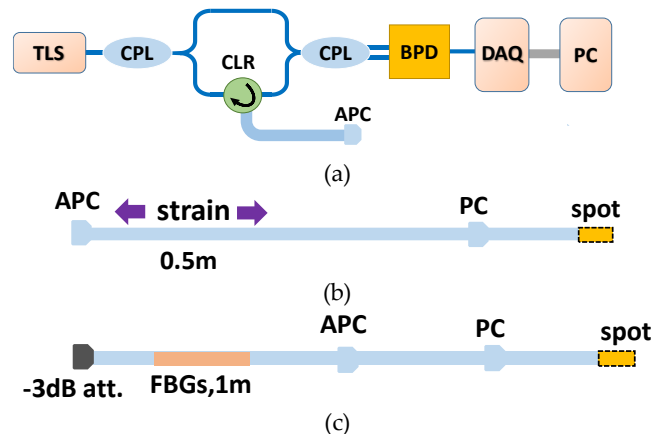


Figure 8. OFDR system using the self-reference for the nonlinearity correction. (a) OFDR interrogation system (b) Configuration 1: all composed by single mode fiber. (c) Configuration 2: The fiber part between the attenuator and the APC connector is a Ge-doped fiber with 1m dense weak FBG arrays inscribed in the middle.

The OFDR system using the self-reference for the nonlinearity correction in this part is similar to the system shown in Figure 3. However, in Figure 8(a), only the main interferometer is kept. The TLS sweeps from 1540 nm to 1560 nm and its nominal tuning speed is 40 nm/s. The sampling rate of data acquisition card (DAQ) is 10 MS/s. Two configurations are investigated. The first is shown in Figure 8(b). All segments are composed by single mode fiber. The second is shown in Figure 8(c). The fiber part between the -3 dB attenuator and the APC connector is a Ge-doped fiber with 1m-length dense weak FBG arrays inscribed in the middle. Each single FBG has a length of 8mm and the gap is 2 mm. The weak FBG arrays are made by the phase mask and UV light. The nominal central wavelength is 1550 nm. A -3 dB attenuator is inserted before the sensing segment to reduce the incident light power. The PC connector in two configurations are used to be the reference reflectivity point in the process of the nonlinearity correction.

First, the spatial resolution tests for these two configurations are performed. The equal phase interval in the self-reference for the nonlinearity correction are all set to $\pi/2$. Figure 9 shows the measured OFDR trace of configuration 1 without nonlinearity correction. The -3 dB width of the PC connector is about 1.5m. Then the band-pass filter shown as the red dashed box in the Figure 9 is used to extract the optical phase information of the laser. The correction process follows the process shown in Figure 6. The corrected OFDR trace is shown in Figure 10. The inset is the reflection of the PC connector. The -3 dB width of the PC connector is about 40 μm , which equals to the Fourier transform-limited spatial resolution. Figure 11 shows the measured OFDR trace of configuration 2 after nonlinearity correction. The left inset in Figure 11 is the -3 dB attenuator. The distance between two APC reflectivity planes is about 2 cm. The right inset in Figure 11 is the beginning of the FBG arrays. It can be seen FBG is about 10 dB higher than the Rayleigh scatter level. The interval and reflectivity strength is even. From the results of the spatial resolution tests, the nonlinearity correction method by self-reference is effective.

Then, the sensing tests are implemented. The nonlinearity compensation is achieved by the self-reference method. Then the distributed strain is measured using the conventional demodulation method demonstrated in [1, 10]. The gauge length is set to be 1 cm. The stretching part is the single

mode fiber with acrylate coating. The sensing fiber is stretched by a nanometer stage shown in Figure 12(a). It can generate a standard strain calculated by $\varepsilon = \Delta L / L$, where ΔL is the elongation length of the fiber and L is the original length. The distributed strain are shown in Figure 12(b). So it is certain that the self-reference method will not influence the classical distributed strain demodulation in OFDR.

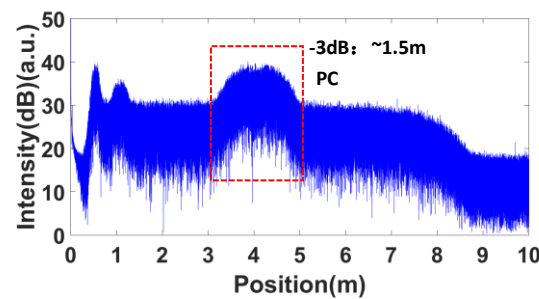


Figure 9. Measured OFDR trace without nonlinearity correction. The -3dB width of the PC connector is about 1.5 m.

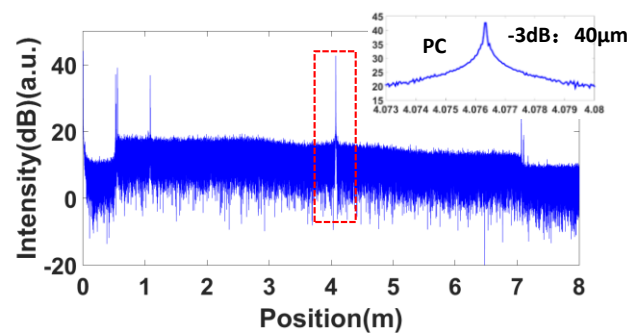


Figure 10. OFDR trace of the configuration 1 with nonlinearity correction. The inset is the reflection of the PC connector.

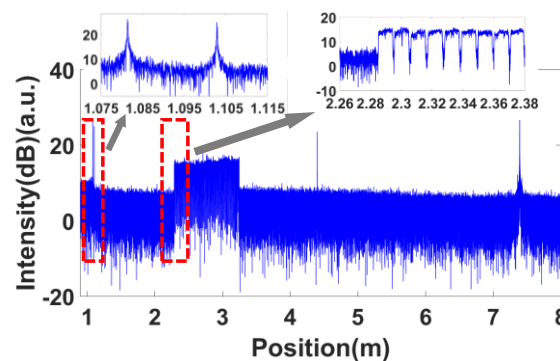
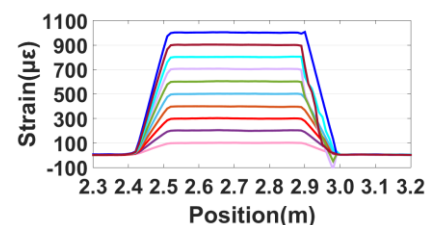


Figure 11. OFDR trace of the configuration 2 with nonlinearity correction.



(a)



(b)

Figure 12. (a) Linear displacement stage to make a certain strain to the fiber. (b) The distributed strain with an increasing strain from 100 $\mu\epsilon$ to 1000 $\mu\epsilon$ with 100 $\mu\epsilon$ interval.

4. Conclusions

In summary, we develop the methods for tuning nonlinearity correction in the OFDR system from the aspects of data acquisition and also the post-processing. From the perspective of principle, these two methods both take advantage of the auxiliary interferometer information to find the equal-spacing frequency position, then trigger the acquisition of the main interferometer or resample the signal of the main interferometer at these equal-spacing frequency positions. The difference is that the former can only trigger the acquisition only at the position of zero-crossing while the latter uses the phase unwrapping to obtain the continuous phase changing of the laser. Therefore, a smaller frequency interval can be set and this will make it possible to achieve the nonlinearity correction for a longer measurable distance. The other difference of these two nonlinearity correction methods is the correction method implemented by the hardware is high-speed and real time. The correction method using the post-processing is not real time, although it can approach to the real time with the usage of a high-performance computing equipment. The advantage of the self-reference lies in that, compared to the conventional post-processing method, the self-reference method can reduce the hardware and data burden for the system and is respected to have a potential value on the system integration and miniaturization.

Author Contributions: S.Z. conceived the research idea, developed the algorithm, performed the experiment and wrote the manuscript. J.C. supervised the research and J.T. reviewed the manuscript.

Funding: This research was funded by National Natural Science Foundation of China under grant number 51575140 and Heilongjiang Province Outstanding Youth Science Fund Project under grant number HSF20190040.

Conflicts of Interest: The authors declare no conflict of interest.

References

1. Froggatt, M.; Moore, J. High-spatial-resolution distributed strain measurement in optical fiber with Rayleigh scatter. *Appl. Opt.* **1998**, *37*, 1735–1740.
2. Gifford, D. K.; Kreger, S. T.; Sang, A. K.; Froggatt, M. E.; Soller, B. J. Swept-wavelength interferometric interrogation of fiber Rayleigh scatter for distributed sensing applications. *Fiber Optic Sensors and Applications V. International Society for Optics and Photonics*. **2007**, 6770: 67700F.
3. Ding, Z.; Wang, C.; Liu, K.; Jiang, J.; Yang, D.; Liu, T. Distributed optical fiber sensors based on optical frequency domain reflectometry: A review. *Sensors*. **2018**, *18*, 1072.
4. Moore, E.D.; McLeod, R. R. Correction of sampling errors due to laser tuning rate fluctuations in swept-wavelength interferometry. *Opt. Express*. **2008**, *16*, 19139–13149.
5. Feng, B.; Liu, K.; Liu, T.; Jiang, J.; Du, Y. Improving OFDR spatial resolution by reducing external clock sampling error. *Opt. Commun.* **2016**, *363*, 74–79.
6. Song, J.; Li, W.; Lu, P.; Xu, Y.; Chen, L.; Bao, X. Long-range high spatial resolution distributed temperature and strain sensing based on optical frequency- domain reflectometry. *IEEE Photonics J.* **2014**, *6*, 1–8.
7. Kim, Y.; Kim, M. J.; Rho, B. S.; Kim, Y. H. Measurement Range Enhancement of Rayleigh-Based Optical Frequency Domain Reflectometry With Bidirectional Determination. *IEEE Photonics J.* **2017**, *9*, 1–8.
8. Gabai, H.; Botsev, Y.; Hahami, M.; Eyal, A. Optical frequency domain reflectometry at maximum update rate using I/Q detection. *Opt. Lett.* **2015**, *40*, 1725–1728.
9. Badar, M.; Lu, P.; Buric, M.; Ohodnicki, R. Self-correction of nonlinear sweep of tunable laser source in OFDR. *Fiber Optic Sensors and Applications XVI*. **2019**, 11000, 1100004.
10. Cui, J.; Zhao, S.; Yang, D.; Ding, Z. Investigation of the interpolation method to improve the distributed strain measurement accuracy in optical frequency domain reflectometry systems. *Appl. Opt.* **2018**, *57*, 1424–1431.